Anion Diffusion | *Very Important Paper* |

And Yet It Moves: A High-Temperature Neutron Diffraction Study of Ion Diffusion in the Inverse Perovskites BaLiX_3 (X = F, H, D)

Dennis Wiedemann,*[a] Eva Maria Heppke,[a] and Alexandra Franz[b]

Abstract: Despite the interest in (anti-)perovskites and diverse hydrides as hydride conductors and all-solid-state battery materials, little experimental evidence on anion diffusion in these compounds is available. Herein, we use neutron diffraction at high temperatures to discover pathways and estimate activation barriers of anion migration in mechanosynthesized powders of BaLiF$_3$, BaLiH$_3$, and BaLiD$_3$. We critically assess the limitations of both current methods for deriving effective one-particle potentials (i.e., via modelling of the probability-density function and via maximum-entropy reconstruction of the scatterer density). The suggested migration pathways run roughly along the edges of the LiX$_6$ octahedra with activation energies of 0.45(3), ca. 0.41, and less than 1.44(3) eV in BaLiD$_3$, BaLiH$_3$, and BaLiF$_3$, respectively. Not only is this the first determination of diffusion barriers in these hydrides but also the second study providing any comparative data on the two methods of derivation.

Introduction

What's in a name? More than just the alphabetical order when it comes to the cations in the title compounds' formulae. Referring to the common perovskite formula ABX_3, the cation with the higher charge, Ba^{2+}, occupies the cuboctahedrally coordinated position A and the cation with the lower charge, Li$^+$, occupies the octahedrally coordinated position B (cf. Figure 1). In analogy to spinels, Roy coined the term "inverse perovskite" for this arrangement.[1] Nevertheless, even sources as popular as the *Wikipedia* fail to discriminate them from "antiperovskites", in which the roles of anions and cations are swapped.[2] The structures of the cubic inverse perovskites BaLiF$_3$, BaLiH$_3$, and BaLiD$_3$ were first elucidated in 1952,[3] 1964,[4] and 1968,[5] respectively. The cell lengths of ca. 3.992 Å and 4.023(1) Å for the fluoride and hydride,[6] reflect the slightly smaller effective radius of F$^-$ ($r_{[6]}$ = 1.33 Å according to Shannon)[7] compared to H$^-$ ($r_{[6]}$ = 1.40 Å according to Gibb).[8] The resulting Goldschmidt tolerance factors t = 0.995 and 0.985 for the inverse arrangement are very similar.[9] For BaLiD$_3$, an intermediate cell length of 4.013(5) Å is reported, which would in turn lead to an inter-

mediate tolerance factor. This is consistent with isotope effects in barium hydrides: The unit cell of BaD$_2$ is slightly smaller than the one of BaH$_2$ with the disparity diminishing for higher temperatures (because of the differences in vibrational energy levels).[10]
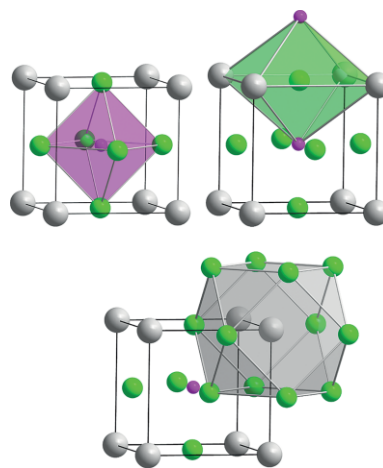

Figure 1. Coordination polyhedra around B = Li (top left), X (top right), and A = Ba (bottom) in the inverse cubic perovskites BaLiX_3. Gray: Ba^{2+}, pink: Li$^+$, green: X^-; ions with arbitrary radii, unit cell in black.

Beginning with the discovery of these compounds, a fluoride–hydride analogy was assumed and later established as a more general crystal-chemical principle:[11] Not only are BaLiX_3 the sole compounds in their ternary systems Ba–Li–X,[12] fluoride and hydride ions are also miscible within pseudo-binary systems like BaF$_2$–BaH$_2$.[13] For BaLiH$_x$F$_{3-x}$ in particular, a narrow miscibility range of $0 < x \leq 0.20$ was proposed,[14] but computations predict the absence of any gap.[15]

[a] *Institut für Chemie, Technische Universität Berlin,*
    Straße des 17. Juni 135, 10623 Berlin, Germany
    E-mail: dennis.wiedemann@chem.tu-berlin.de
    http://dennis.wiedemann.name
[b] *Abteilung Struktur und Dynamik von Energiematerialien,*
    Helmholtz-Zentrum Berlin für Materialien und Energie,
    Hahn-Meitner-Platz 1, 14109 Berlin, Germany
    Supporting information and ORCID(s) from the author(s) for this article are
    available on the WWW under https://doi.org/10.1002/ejic.201901232.

★ ChemPubSoc
Europe

EurJIC
European Journal
of Inorganic Chemistry

Communication

While there is ongoing scientific and commercial interest in BaLiF$_3$ (e.g., most recently as host for luminescent lanthanoid[16] and actinoid ions[17] and as antisite defect material[18]), less attention is paid to BaLiH$_3$ – probably because of its air sensitivity. [Understandably, the more expensive BaLiD$_3$ was only used for sparse neutron diffraction/scattering studies connected to structure elucidation[5] and luminescence of guest europium(II) ions.[19]] The resulting scarcity of data on ion migration in pure perovskite hydrides is unfortunate, especially in light of the current hot topic of (anti-)perovskites[20] and structurally diverse hydrides[21] as hydride conductors and (all-solid-state) battery materials. A recent quasi-elastic neutron scattering (QENS) study on hydride diffusion in hydride-doped oxide perovskites showed that migration pathways—even in simple materials—are not always straightforward: It identified two different diffusion pathways, the interplay of which depends on temperature.[22]

Herein, we report on powder neutron diffractometry of BaLiX_3 (X = F, H, D) carried out at the FIREPOD (E9) instrument at Helmholtz-Zentrum Berlin.[23] Diffusion pathways with their associated bottlenecks and activation barriers (derived using our own tool CalcOPP)[24] are identified and compared to published results from topology and bond-valence energy landscape (BVEL) analyses of O:BaLiF$_3$ single crystals.[25]

Results and Discussion

Instead of fusing salts or hydrogenating alloys,[19] we successfully synthesized phase-pure BaLiX_3 samples mechanochemically from BaX_2 and LiX powders (see Supporting Information). While BaLiF$_3$ was stable at 500 °C and 700 °C, the hydrides decomposed at the latter temperature (see Figures S1–S7 and Figures S8–S10 for diffractograms and derived crystal structures, respectively). CSD 1965603 (for BaLiH$_3$ at 25 °C), 1965604 (for BaLiH$_3$ at 500 °C), 1965605 (for BaLiF$_3$ at 700 °C), 1965606 (for BaLiF$_3$ at 25 °C), 1965607 (for BaLiD$_3$ at 500 °C), 1965608 (for BaLiF$_3$ at 500 °C), and 1965609 (for BaLiD$_3$ at 25 °C) contain the supplementary crystallographic data for this paper. These data can be obtained free of charge from FIZ Karlsruhe via FIZ Karlsruhe.

In the time- and space-averaged picture of neutron diffractometry, ionic motion manifests as "smearing" of scattering-length density (SLD) along the diffusion pathway. This can be modelled using displacement parameters including anharmonic terms, which leads to the probability-density function (PDF) of finding an ion displaced to a certain position. Alternatively, it can be mapped directly using reconstruction via maximum-entropy methods (MEM) to minimize artefacts. (For a detailed discussion, see ref.[26]) Heeding certain caveats,[27] one can use both methods to derive the effective one-particle potential (OPP) describing the energy landscape experienced by the ion in motion.[28] While the former approach may lead to incomplete modelling of the SLD (and thus overestimation of the OPP), the latter offers neither assignment of the SLD to a specific ion (and may thus lead to a "tainting" of the OPP by neighboring atoms) nor calculation of uncertainties.

When modelling the anion PDF in BaLiF$_3$, we found considerable (probably static) disorder at r.t. that manifests in anhar-

monic displacement. Its features change gradually up to 700 °C, where a path between neighboring anion positions runs roughly along the edges of the LiX_6 octahedron with the bottleneck in the center (see Figure 2, top). In BaLiD$_3$, no static disorder was found at room temperature, but ample dynamic effects were present at 500 °C. The pathway is comparable to the one in BaLiF$_3$ but with the bottleneck somewhat nearer to the lithium ion (see Figure 2, bottom). For BaLiH$_3$, the intrinsically high background due to incoherent scattering led to a low signal-to-noise ratio. We thus found a refinement including a large number of anharmonic terms (as would have been necessary for enhancement) unwarranted and refrained from it.
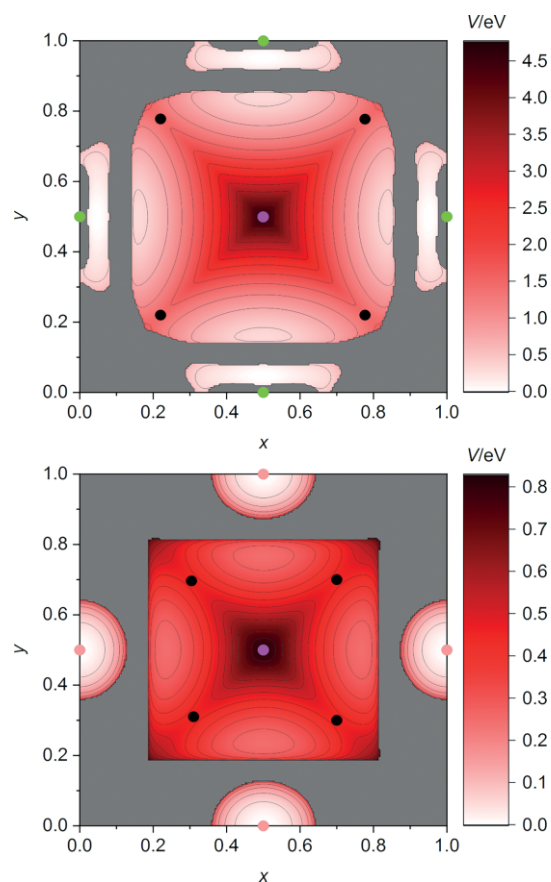

Figure 2. Section through the PDF-derived anion OPP V at $z = \frac{1}{2}$ in BaLiF$_3$ at 700 °C (top; contours: $V_0 = 0$, $\Delta V = 0.375$ eV) and in BaLiD$_3$ at 500 °C (bottom; contours: $V_0 = 0$, $\Delta V = 0.055$ eV). Reference positions marked as dots (pink: Li$^+$, green: F$^-$, coral: D$^-$, black: bottlenecks), areas of formally infinitely high potential in gray.

The OPPs directly derived from MEM-reconstructed SLDs (see Figure 3) show a similar pathway for BaLiH$_3$, in which the anion carries a negative scattering length. For BaLiF$_3$ and BaLiD$_3$, containing an anion with a positive scattering length, a curved pathway with the bottleneck on or near the center of a LiF$_6$ face is indicated. In all three cases, the OPPs at the bottleneck level elevated by 3σ (as derived from PDF modelling) show that barium-associated positive SLD, probably caused by vibrations or local jumps, is present around the position $\frac{1}{3}$, $\frac{1}{3}$, $\frac{1}{3}$. Thus, the pathways must be considered tainted for BaLiF$_3$ and BaLiD$_3$, whereas BaLiH$_3$ (with the proton a negative scatterer) is not susceptible to this systematic error.
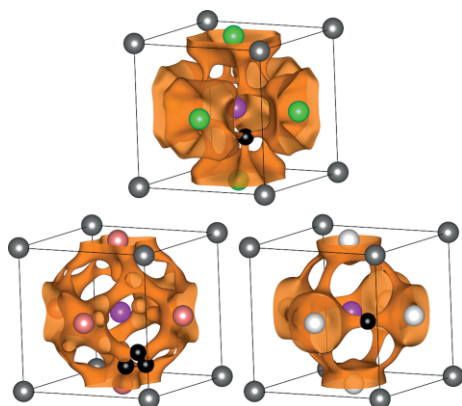
ChemPubSoc
Europe

EurJIC
European Journal
of Inorganic Chemistry

Communication

Figure 3. Anion OPPs as derived from MEM-reconstructed SLD in $BaLiF_3$ at 700 °C (top, $V = 0.58$ eV), in $BaLiD_3$ at 500 °C (bottom left, $V = 0.37$ eV), and in $BaLiH_3$ at 500 °C (bottom right, $V = 0.41$ eV). Orange: OPP isosurface, gray: Ba^{2+}, pink: Li^+, green: F^-, coral: D^-, white: H^-, black: exemplary bottleneck positions; ions with arbitrary radii, unit cell in black.

The activation barrier for migration is the maximal OPP along the path, i.e., at the bottleneck position (see Table 1).[29] For $BaLiF_3$, the values according to the two methods differ strongly. Whereas the PDF-derived pathway is in tune with findings from topological and BVEL analyses,[25] the activation barrier seems too high compared to ca. 0.64 eV (BVEL) and 1.04(3) eV (conductometry of annealed powders).[30] This is probably due to incomplete modelling of the fluoride-associated SLD. Interestingly, for $BaLiD_3$, the values connected to different pathways are equal within 3σ. The preferable, PDF-derived value for $BaLiD_3$ is close to the barrier derived from SLD for $BaLiH_3$—as expected for isotopomers.

Table 1. Activation barriers (in eV) and bottleneck positions (in parentheses) for anion migration in $BaLiX_3$ (bold: preferable values; see text).

	$BaLiF_3$	$BaLiD_3$	$BaLiH_3$
ϑ/°C	700	500	500
From PDF	**1.44(3)**	**0.45(3)**	—[a]
	(½, **0.22**, **0.22**)	(½, **0.30**, **0.30**)	
From SLD	0.58	0.37	**0.41**
	(⅓, ⅓, ⅓)	(0.29, 0.19, 0.19)	(½, **0.19**, **0.19**)

[a] Evaluation of anharmonic displacement not warranted by data quality.

Of course, migration can only occur from an occupied anion position to a vacancy defect. With the concentration of such defects, the jump (attempt) frequency, as quantified in the pre-exponential factor of a typical Arrhenius model for activation, increases. For a determination via neutron diffractometry, jumps have to be frequent lest the barriers are overestimated or diffusion even becomes invisible. In $BaLiF_3$ powders, jumps occur less often in the following sequence: mechanosynthesized, additionally annealed, solid-state synthesized.[30] This means that the jump frequency decreases with crystallite size and perfection—explaining why we previously had been unsuccessful in mapping diffusion pathways in a single crystal.[25]

Conclusions

The pathway for thermally activated anion diffusion in $BaLiX_3$ runs between adjacent anion positions roughly along the edges of the lithium coordination octahedron. For $X = H$, this was deduced directly from the MEM-reconstructed SLD. For $X = D$, F, the influence of barium-ion dynamics made a partitioning via anion PDF modelling necessary. The associated activation barriers for migration are 0.45(3) and ca. 0.41 eV for $BaLiD_3$ and $BaLiH_3$, respectively. The value of 1.44(3) eV for $BaLiF_3$ must be considered as a least upper bound because of possible overestimation. Nonetheless, a higher barrier for fluoride compared to the hydrides is expected because of the higher polarizability and thus enhanced steric adaptability of the latter.[11a]

The determined anion path conforms to the vacancy migration mechanism accepted for oxide perovskites.[31] Then again, we have not found evidence for a prevalent pathway between next-nearest positions (i.e., through the center of a unit-cell edge) as was reported for hydride ions in $BaTiO_{3-x}H_x$ above 400 K.[22] Unfortunately, a systematic and thorough comparison of PDF-derived and SLD-derived ion pathways / migration barriers is still lacking, making this work and our study on Na_xTiS_2[27] the hitherto only examples available.

[1] R. Roy, *J. Am. Ceram. Soc.* **1954**, *37*, 581–588.
[2] Wikipedia contributors, "Antiperovskite (structure)", to be found under https://en.wikipedia.org/w/index.php?title=Antiperovskite_(structure)&oldid=902844119, **2019**.
[3] W. L. W. Ludekens, A. J. E. Welch, *Acta Crystallogr.* **1952**, *5*, 841.
[4] C. E. Messer, J. C. Eastman, R. G. Mers, A. J. Maeland, *Inorg. Chem.* **1964**, *3*, 776–778.
[5] A. J. Maeland, A. F. Andresen, *J. Chem. Phys.* **1968**, *48*, 4660–4661.
[6] The term "hydride" denotes the title compound containing hydrogen in its natural mixture, whereas "deuteride" refers to the isotopically substituted compound containing only hydrogen-2. "Hydrides" is used as an umbrella term for both compounds.
[7] R. D. Shannon, *Acta Crystallogr., Sect. A* **1976**, *32*, 751–767.
[8] T. R. P. Gibb Jr., in *Progress in Inorganic Chemistry, Volume III* (Ed. F. A. Cotton), Interscience Publishers, New York, **1962**, pp. 315–509.
[9] V. M. Goldschmidt, *Naturwissenschaften* **1926**, *14*, 477–485.
[10] V. P. Ting, P. F. Henry, H. Kohlmann, C. C. Wilson, M. T. Weller, *Phys. Chem. Chem. Phys.* **2010**, *12*, 2083–2088.
[11] a) C. E. Messer, *J. Solid State Chem.* **1970**, *2*, 144–155; b) A. J. Maeland, W. D. Lahar, *Z. Phys. Chem.* **1993**, *179*, 181–185.
[12] C. E. Messer, I. S. Levy, *Inorg. Chem.* **1965**, *4*, 543–548.
[13] J.-F. Brice, M. Perrin, R. Leveque, *J. Solid State Chem.* **1979**, *30*, 183–188.
[14] M. Kamata, A. Matsumoto, T. Esaka, *Denki Kagaku oyobi Kogyo Butsuri Kagaku* **1998**, *66*, 443–445.
[15] N. Kunkel, H. Kohlmann, *J. Phys. Chem. C* **2016**, *120*, 10506–10511.
[16] J. Christmann, H. Hagemann, *J. Phys. Chem. A* **2019**, *123*, 2881–2887.
[17] S. J. Camardello, A. A. Setlur (General Electric Company, USA), WO **2019**/060055 A2, **2019**.
[18] a) A. Düvel, L. M. Morgan, C. V. Chandran, P. Heitjans, D. C. Sayle, *Cryst. Growth Des.* **2018**, *18*, 2093–2099; b) A. Düvel, L. M. Morgan, G. Cibin, D. Pickup, A. V. Chadwick, P. Heitjans, D. C. Sayle, *J. Phys. Chem. Lett.* **2018**, *9*, 5121–5124.

[19] a) N. Kunkel, A. Meijerink, H. Kohlmann, *Phys. Chem. Chem. Phys.* **2014**, *16*, 4807–4813; b) N. Kunkel, R. Böttcher, T. Pilling, H. Kohlmann, A. Pöppl, *Z. Phys. Chem.* **2016**, *230*, 931–942; c) N. Kunkel, A. D. Sontakke, S. Kohaut, B. Viana, P. Dorenbos, *J. Phys. Chem. C* **2016**, *120*, 29414–29422; d) G. Lefevre, A. Herfurth, H. Kohlmann, A. Sayede, T. Wylezich, S. Welinski, P. Duarte Vaz, S. F. Parker, J. F. Blach, P. Goldner, N. Kunkel, *J. Phys. Chem. C* **2018**, *122*, 10501–10509; e) T. Wylezich, R. Böttcher, A. D. Sontakke, V. Castaing, B. Viana, A. Pöppl, N. Kunkel, *J. Phys. Chem. C* **2019**, *123*, 5031–5041.

[20] a) K. T. Lai, I. Antonyshyn, Y. Prots, M. Valldor, *J. Am. Chem. Soc.* **2017**, *139*, 9645–9649; b) C. Berger, E. Bucher, A. Windischbacher, A. D. Boese, W. Sitte, *J. Solid State Chem.* **2018**, *259*, 57–66.

[21] a) G. Kobayashi, Y. Hinuma, S. Matsuoka, A. Watanabe, M. Iqbal, M. Hirayama, M. Yonemura, T. Kamiyama, I. Tanaka, R. Kanno, *Science* **2016**, *351*, 1314–1317; b) Y. Iwasaki, N. Matsui, K. Suzuki, Y. Hinuma, M. Yonemura, G. Kobayashi, M. Hirayama, I. Tanaka, R. Kanno, *J. Mater. Chem. A* **2018**, *6*, 23457–23463; c) K. Fukui, S. Iimura, T. Tada, S. Fujitsu, M. Sasase, H. Tamatsukuri, T. Honda, K. Ikeda, T. Otomo, H. Hosono, *Nat. Commun.* **2019**, *10*, 2578.

[22] C. Eklöf-Österberg, R. Nedumkandathil, U. Häussermann, A. Jaworski, A. J. Pell, M. Tyagi, N. H. Jalarvo, B. Frick, A. Faraone, M. Karlsson, *J. Phys. Chem. C* **2019**, *123*, 2019–2030.

[23] Helmholtz-Zentrum Berlin für Materialien und Energie, *J. Large-Scale Res. Facil.* **2017**, *3*, A103; https://doi.org/110.17815/jlsrf-17813–17127.

[24] D. Wiedemann, CalcOPP, Calculation of One-Particle Potentials, Technische Universität Berlin, Berlin, Germany, **2019**; https://doi.org/10.5281/zenodo.2530345.

[25] D. Wiedemann, F. Meutzner, O. Fabelo, S. Ganschow, *Acta Crystallogr., Sect. B: Struct. Sci. Cryst. Eng. Mater.* **2018**, *74*, 643–650.

[26] D. Wiedemann, M. M. Islam, T. Bredow, M. Lerch, *Z. Phys. Chem.* **2017**, *231*, 1279–1302.

[27] D. Wiedemann, E. Suard, M. Lerch, *RSC Adv.* **2019**, *9*, 27780–27788.

[28] S. Strangmüller, H. Eickhoff, D. Müller, W. Klein, G. Raudaschl-Sieber, H. Kirchhain, C. Sedlmeier, V. Baran, A. Senyshyn, V. L. Deringer, L. van Wüllen, H. A. Gasteiger, T. F. Fässler, *J. Am. Chem. Soc.* **2019**, *141*, 14200–14209.

[29] Please note that this barrier does not take the energy of defect formation into account, which is, for example, included in conductometry or tracer-diffusion experiments.

[30] A. Düvel, M. Wilkening, S. Wegner, A. Feldhoff, V. Šepelák, P. Heitjans, *Solid State Ionics* **2011**, *184*, 65–69.

[31] R. J. D. Tilley, in *Perovskites: Structure–Property Relationships*, John Wiley & Sons, **2016**, pp. 158–175.